RESEARCH OPEN ACCESS

Journal of Venomous Animals and Toxins including Tropical Diseases

ISSN 1678-9199

www.jvat.org

Compositional and toxicological investigation of pooled venom from farm-raised *Naja atra*

Gang Xiao[1,2], Junqi Liu[1,3], Lingfeng Peng[1,2], Yang Yang[1], Zhiliang Sun[1,2*]

[1]College of Veterinary Medicine, Hunan Agricultural University, Changsha, Hunan, China.
[2]Hunan Engineering Research Center of Veterinary Drug, Hunan Agricultural University, Changsha, Hunan, China.
[3]Veterinary Drug Laboratory, Hunan Institute of Animal and Veterinary Science, Changsha, Hunan, China.

Abstract

Background: *Naja atra* is a venomous snake species medically relevant in China. In the current study, we evaluated the composition and toxicological profile of venom collected from farm-raised *N. atra*.

Methods: Venom was collected from third-generation captive bred *N. atra* on a snake farm in Hunan Province, China. The venom was analyzed using sodium dodecyl sulfate polyacrylamide gel electrophoresis and nano-liquid chromatography with electrospray ionization tandem mass spectrometry. In addition, hemolytic activity, median lethal dose, serum biochemical and histopathological parameters were accessed.

Results: *N. atra* venom proteome was dominated by phospholipase A_2 (46.5%) and three-finger toxins (41.4 %), and a set of common low relative abundance proteins, including cysteine-rich secretory proteins (4.7%), NGF-beta (2.4%), snake venom metalloproteinase (1.5%), glutathione peroxidase (0.6%), vespryn (0.3%), and 5'-nucleotidases (0.2%) were also found. Furthermore, the venom exhibited direct hemolytic activity, neurotoxicity, myotoxicity, and high lethal potency in mice, with a subcutaneous median lethal dose of 1.02 mg/kg. Histopathological analysis and serum biochemical tests revealed that venom caused acute hepatic, pulmonary and renal injury in mice.

Conclusion: This study revealed the composition and toxicity of venom collected from farm-raised *N. atra*, thereby providing a reference for the analysis of venom samples collected from captive-born venomous snakes in the future.

Keywords:
Naja atra
Phospholipase A_2
Three-finger toxins
Neurotoxicity
Myotoxicity

*** Correspondence:** sunzhiliang1965@aliyun.com
https://doi.org/10.1590/1678-9199-JVATITD-2021-0040
Received: 05 April 2021; Accepted: 30 August 2021; Published online: 14 March 2022

Background

China possesses an extremely rich and diverse snake fauna, consisting of approximately 209 known species of land and sea snakes. Of these, Chinese cobra *(Naja atra)*, ranked as one of the top ten venomous snakes in the country, is considered one of the most medically important snake species [1]. To meet the increasing demand for snakes and their products, as well as to protect wild snake resources, farm breeding or snake farming is conducted to breed snakes of economic and medical relevance, such as *N. atra*. In Hunan Province, China, farm-raised venomous snakes are a stable source of venom used to produce cosmetics and snake venom hemagglutinase injections.

N. atra belongs to the Elapidae family, whose members contain venom that induces neurotoxic, hemolytic, proteolytic, hemorrhagic, and necrotizing activities in experimental models [1–3]. Patients bitten by *N. atra* usually develop necrosis, tremors, blurred vision, tachypnea, arrhythmia, and rarely hemorrhage. Victims may also suffer from acute respiratory, circulatory and renal failure [4]. Recently, several novel proteins with important biological activities have been characterized and isolated from this venom. For example, α-elapitoxin-Na1a, a novel short-chain postsynaptic neurotoxin, was isolated from *N. atra* venom and exhibits relatively strong binding activity with the skeletal muscle nicotinic acetylcholine receptor (nAChR) [5]. Moreover, atrase B, a novel metalloproteinase isolated from *N. atra* venom, may be a potential adjuvant therapeutic drug with application in xenotransplantation owing to the dual anti-complement and anti-coagulation activities [6].

Studies [7,8] have previously analyzed the protein composition of *N. atra* venom from Zhejiang and Taiwan, China, and have identified three-finger toxins (3FTx) and phospholipase A_2 (PLA_2) as the main components of this venom. Jiang et al. [9]. found that the venom transcriptome of *N. atra* from Zhejiang mainly contains 3FTxs, exhibiting cytotoxicity and neurotoxicity (short chain α-NTX). Moreover, Li et al. [10] assessed the venom proteomic profiles from *N. atra* from Yiwu County, Zhejiang Province, China using four different approaches. Furthermore, previous studies have reported geographic and age-related variations in the proteome and enzymatic and toxicological activities of *N. atra* venom [4,8,11]. Gao et al. [11] found that venom yield of *N. atra* was related to the gender, age and geographic location.

Studies of other snake species have found differences between venom collected from snakes in captivity and in the wild [12]. Intraspecific variation in venom composition is an important cause of differences in venom function and the clinical pathophysiology of envenomation [13–16]. However, the current critical problem is that the knowledge of venom proteins in snakes from completely different regions is incomplete, and the clinical pathophysiology of patients envenomed by *N. atra* from completely different regions remain unknown. Proteomic approach has been used to characterize *Naja* venoms [17]. Therefore, it is necessary to study the venom proteome, toxicological activities and pathophysiology of *N. atra* from vital areas that include key habitats of this snake.

In the present study, we investigated the venom proteome and toxicity of farmed *N. atra* venom in Hunan Province, China. Our results provide important information on the composition and activities of *N. atra* venom from this province.

Methods

Snakes

The snakes from which venom samples were collected from third-generation *Naja atra* captive bred on the Hunan Yongzhou Yishe Science and Technology Industrial, Lingling District, Yongzhou City, Hunan Province, China. The snakes were all hatched at the same time, and the feeding environment and other aspects in the later feeding process were the same for all specimens. The average weight of the snakes was 1.5 kg, with an approximate age of one year. A total of 20 snakes (10 females and 10 males) were maintained at constant temperature and humidity conditions (25 °C, 60%) and fed with thawed rodents.

Snake venom

Snakes were provided with water for a week before venom collection; during this period, food was not provided to the snakes. Venom extraction was performed during July-August in a glass beaker covered with a thick plastic sheet and immersed in an ice bath. July-August was the peak period for venom collection in the snake farm, and the interval between each collection was 25 days. The freshly collected venom samples was pooled, freeze-dried in a vacuum dryer and stored at -20 °C.

Mammals and reagents

Male and female Kunming mice (20 ± 0.7 g; licensed: SCXK [Xiang] 2016-0002) and rabbits (male; approximate weight: 2.0 kg) were purchased from Hunan SJA Laboratory Animal, Hunan, China. Kits (batch number: 2200424) for analysis of serum creatinine (SCR), urea nitrogen (UN), aspartate aminotransferase (AST), alanine aminotransferase (ALT), and creatine kinase (CK) levels were purchased from Jiangsu Sinnowa Medical Science & Technology, Jiangsu, China. Sodium dodecyl sulfate polyacrylamide gel electrophoresis (SDS-PAGE) gels were purchased from Sigma-Aldrich (St. Louis, MO, USA), and protein endonuclease trypsin (sequencing grade) was purchased from Promega (Madison, WI, USA). Other chemicals for proteolysis were purchased from Sigma-Aldrich.

SDS-PAGE

SDS-PAGE was done as described by Laemmli [18]. The Spectra Multicolor Broad Range Protein Ladder (11–245 kDa) (Beijing Solarbio Science &Technology, Beijing, China) was used for calibration. Crude venom (20 μg) was loaded onto a 15% gel,

and electrophoresis was performed under reducing conditions at 75 V for 30 min, followed by 110 V for 2 h. Subsequently, the gels were stained with Coomassie Brilliant Blue R-250 (Beijing Solarbio Science &Technology, Beijing, China) and the protein bands were visualized and documented using a gel imaging system (Bio-Rad, USA).

Identification of *N. atra* venom proteins

Sample preparation

Venom was dissolved in ultrapure water and the concentration was adjusted to 1 mg/mL. Subsequently, the sample was centrifuged (3,000 × *g;* 10 min, 4 °C), and the supernatant was used for further analysis. Venom samples were subjected to treatments as per protocols described by Shevchenko et al. [19]. The sample solution was first denatured in 8 M urea, the disulfide linkages were reduced with 10 mM dithiothreitol, and all cysteine residues were alkylated using 55 mM iodoacetamide in the dark at 37 °C for 45 min. The sample was then subjected to cleaning in a C18-based spin column (Thermo Fisher, USA) and was digested using sequencing-grade modified trypsin (Promega, USA) with a digestion buffer (ammonium bicarbonate 100 mM, pH 8.5). The peptides obtained after digestion were dried in a Speed Vac dryer (Thermo Fisher, USA). The dried sample was then resuspended in 2% acetonitrile, 97.5% water, and 0.5% formic acid and analyzed using the nano-LC-ESI-MS/MS system.

Nano-liquid chromatography-electrospray ionization-mass spectrometry (nano-LC-ESI-MS/MS) analysis

Nano-LC-ESI-MS/MS analysis of the digested protein samples was performed using a high-pressure liquid chromatography (HPLC) system (Agilent, USA) with a reverse phase C18 column (inner diameter: 75 μm; length: 8 cm; particle size: 3 μM; and pore size: 300 Å). The injection time was 20 min. HPLC solvent A comprised 97.5% water, 2% acetonitrile, and 0.5% formic acid, and solvent B contained 9.5% water, 90% acetonitrile, and 0.5% formic acid. The time required for the gradient to run from 2% solvent B to 90% solvent B was 60 min, in addition to 20 min for sample loading and 20 min for column washing. The column flow rate was approximately 800 nL/min after the completion of splitting, and the typical injection volume was 3 μL.

The HPLC system was coupled to an LTQ linear ion trap mass spectrometer (Thermo, USA) such that the sample eluted from the HPLC column was directly subjected to ionization by ESI before sample entry into the mass spectrometer. The ionization voltage was optimized before the conduction of every step and maintained within a range of 1.2–1.8 kV. The capillary temperature was set at 110 °C. The mass spectrometer was used in a data-dependent mode to acquire MS/MS data via a low-energy collision-induced dissociation (CID) process. The default collision energy was 33% and the default charge state was 3. One full scan using a microscan with a mass range of 550–1800 Da was acquired; subsequently, one MS/MS scan of the most intense ion was acquired, which included a full mass range and three microscans. The dynamic exclusion feature was set as follows: repeat count of 1 within 0.3 min and exclusion duration of 0.4 min. The exclusion width was 4 Da.

Database search and validation

Mass spectrometric data were used to search against the UniProt protein database with ProtTech's ProtQuest software suite (Norristown, PA, USA). The parameters for data acquisition and processing were as follows. Data acquisition parameters: instrument, LTQ; software, Xcalibur 2.0; and centroid mode minimum MS signal for precursor ion: 5×10^4 counts. Data processing parameters: software, ProtQuest 2.0; signal-to-noise-ratio, ≥ 5; De-isotoped, yes; filtered, yes; missed cleavages, ≤ 5; modifications, Cys +57; and database, Serpentes protein database from UniProt (accession date: November 23, 2018). Validation parameters: for proteins identified based on 1 peptide (score ≥ 15); for proteins identified with more than 1 peptide (score ≥ 13).

Protein quantitation

Protein abundance was calculated using the label-free protein quantitation method described by Griffin et al. [20]. The scoring function was based on the MS abundance recorded in both MS and MS/MS data sets, spectral count (SC; number of MS/MS spectra per peptide), non-duplicate peptide number (PN), and fragment ion (MS/MS) intensities. The normalized spectral index (SI_N) was calculated for venom solution using the following equation:

$$SI_N = \left[\sum_{k=1}^{pn}\left(\sum_{j=1}^{sc} i_j\right)_k\right] \Big/ \left[\sum_{j=1}^{n} SI_j\right] \Big/ L$$

where *pn* represents the PN, *sc* represents the SC, *i* represents the fragment ion intensity of peptide k, *j* represents the jth spectral count of sc total spectral counts for peptide k, *n* represents the total number of proteins identified, and *L* represents the number of amino acids in a protein.

Hemolytic activity

The *in vitro* hemolytic activity of the venom was determined as described by Accary et al. [21], with slight modifications. Blood was collected from healthy rabbits into tubes without anticoagulant, and the erythrocytes were separated by centrifugation (2,000 × *g*, 5 min). Before analysis, the erythrocytes were washed three times with normal saline and then incubated with increasing normal saline. The erythrocytes were prepared as described above and aliquots were incubated with increasing concentrations (10–100 μg/mL) of venom for 60 min, after which the tubes were

centrifuged and the absorbance of the supernatant read at 530 nm. The extent of hemolysis was expressed as a percentage of the absorbance obtained by incubating erythrocytes with distilled water (positive control, 100%). The negative control consisted of erythrocytes incubated with 0.9% saline alone.

Venom lethality

Mice were injected subcutaneously with venom at doses of 0.5, 0.7, 1.1, 1.7 and 2.5 mg/kg (10 mice/dose) in the dorsal region of the neck in a fixed volume of 100 uL of saline solution. The general condition of the mice, including the manifestations of envenomation and number of deaths, was monitored over the next 24h, during which the animals had free access to food and water. All mice were necropsied to assess the internal venom-induced pathological alterations. The median lethal dose (LD_{50}) was calculated using probit analysis [22].

Histopathological analysis

Kunming mice were subcutaneously injected with an LD_{50} of venom. Randomly selected mice were killed by cervical dislocation at 6, 12, and 24h (n = 3), and their liver, lungs, kidneys, and heart were dissected immediately and fixed using a fixative solution (Wuhan Servicebio Science &Technology, Beijing, China). Tissue sections 5 μm thick [Indicate thickness] were stained with hematoxylin and eosin (H&E) and examined under a microscope.

Serum biochemical tests

Kunming mice were injected s.c. with one LD_{50} of venom whereas control mice received the same volume of saline. When the venom-injected mice showed signs of envenomation (~1 h after injection), blood samples were collected from the orbital plexus into tubes without anticoagulant and the mice then killed by cervical dislocation. The blood samples were centrifuged (2,800 x g, 4 °C) and the resulting serum was used for the quantification of ALT, AST, UN, SCr and CK using commercial assay kits.

Statistical analysis

Experimental data are presented as mean ± SEM. Statistical analyses were performed using the GraphPad Prism 5 software (La Jolla, CA, USA). Two-tailed Student's *t*-test and analysis of variance were used to analyze different groups, with $P < 0.05$ indicating significance.

Results

Characterization of *N. atra* venom proteome

Figure 1A illustrates the protein components in venom based on 15% SDS-PAGE under reducing conditions. An intense low-molecular-weight protein band at < 15 kDa, as well as multiple protein bands with molecular weights ranging from 40 kDa to > 100 kDa, could be observed. To identify the major protein components in *N. atra* venom samples, we conducted a comprehensive proteomic analysis using nano-LC-ESI-MS/MS. A total of 47 different proteins were identified in the venom, belonging to 21 protein families (Table 1); the main toxin protein families were PLA_2 (45.6%), 3FTx (41.4%), CRISP (4.7%), NGF-beta family (2.4%), and SVMP (1.5%) (Figure 1B). Additional file 1 shows more detailed data on such proteins.

Lethality and hemolytic activity of *N. atra* venom

Table 2 and Figure 2 shows the data on lethality and hemolytic activity of *N. atra* venom, respectively. The LD_{50} for Kunming mice injected subcutaneously with venom was 1.02 mg/kg, the 95% confidence interval was 0.82-1.22 mg/kg, and the clinical symptoms were muscle weakness and respiratory paralysis. As shown in Figure 2, a venom concentration of 100 ug/mL caused 32% hemolysis in rabbit erythrocytes.

Histological analysis of tissue damage

Tissue sections of vital organs were stained with hematoxylin-eosin for histological analysis of venom-induced tissue damage (Figure 3). Hepatic tissues in the control groups exhibited normal cellular structures with distinct hepatic cells, hepatic portal canals, and bile ducts. However, in the experimental groups, inflammatory infiltrate (at 6h), cell border obscurity, and hepatocyte necrosis (at 12h and 24h) were clearly distinguishable. The renal tissues in the control group showed no histological abnormalities, whereas those in the experimental groups showed histological alterations such as the formation of glomerular and renal cysts (at 6h), proteinaceous material deposition in renal tubules (at 12h), epithelial cells of renal tubule edema, and cytoplasmic vacuolation (at 24h). The pulmonary tissues of control mice showed the presence of homogeneous air sacs and alveolar septa, as observed in normal lungs. However, histological alterations were noted in the lung tissues of experimental mice, including hyperplasia of peripheral lymphoid tissues and perivascular edema (at 6h), alveolar fusion, thickening and rupture of alveolar walls, and pulmonary interstitial edema (at 12h and 24h). Heart tissues of envenomed mice showed muscle fiber degeneration (see Additional file 2).

Serum biochemical parameters

Significant increases were noted in the serum biochemical parameters of venom-injected mice compared to saline-treated (control) mice. The parameters indicative of hepatic function are shown in Figure 4A–4B: AST and ALT activities were markedly higher in the experimental group than those observed in the control group. The levels of serum UN and SCr, which are important indices of renal function, have been presented in Figure 4C–4D. CK activity, a biomarker for systemic myotoxicity, was significantly higher in envenomed miced than in the control group (Figure 4E). These parameters were markedly higher in the experimental group than those observed in the control group.

Table 1. Summary of venom proteins of *N. atra* assigned by protein families.

Family	Protein name	Protein mass (kDa)	Source organism	Database accession	Length	No. of peptide	No. of non-duplicate peptide	Probability	Score	Relative abundance (%)
PLA_2	Acidic phospholipase A_2 natratoxin	14.0	*Naja atra*	A4FS04	119	188	10	99.0%	2745	46.5
3FTx	Cytotoxin KJC3	7.2	*Naja sputatrix*	P60311	60	91	8	99.0%	1010	21.0
3FTx	Neurotoxin homolog NL1	10.5	*Naja atra*	Q9DEQ3	86	14	4	99.0%	227	1.3
3FTx	Long neurotoxin 3	8.4	*Naja naja*	P25671	71	8	3	99.0%	108	2.1
3FTx	Neurotoxin 3	7.4	*Naja sputatrix*	Q9PSN6	62	29	4	99.0%	319	6.3
3FTx	Cobrotoxin-b	7.4	*Naja kaouthia*	P59275	61	14	4	99.0%	203	0.5
3FTx	Cytotoxin-like basic protein	7.5	*Naja naja*	P62377	62	7	3	99.0%	93	0.6
3FTx	Muscarinic toxin-like protein 2	7.7	*Naja kaouthia*	P82463	65	14	7	99.0%	210	2.2
3FTx	Weak toxin S4C11	8.0	*Naja melanoleuca*	P01400	65	6	2	96.9%	66	0.2
3FTx	Weak toxin CM-9a	8.0	*Naja kaouthia*	P25679	64	22	1	84.5%	277	5.3
3FTx	Weak neurotoxin 6	10.4	*Naja sputatrix*	O42256	86	46	4	99.0%	534	1.1
3FTx	Muscarinic toxin-like protein 1	7.8	*Naja kaouthia*	P82462	65	9	4	99.0%	109	0.7
CRISP	Cysteine-rich venom protein kaouthin-2	27.1	*Naja kaouthia*	P84808	238	40	10	99.0%	587	0.7
CRISP	Cysteine-rich venom protein kaouthin-1	27.8	*Naja kaouthia*	P84805	239	35	10	99.0%	501	2.2
CRISP	Cysteine-rich venom protein (Fragment)	39.1	*Naja naja*	P86543	33	22	3	99.0%	289	1.4
CRISP	Cysteine-rich venom protein TRI1 (Fragment)	27.5	*Trimorphodon biscutatus*	Q2XXP4	236	2	1	85.9%	24	<0.1
CRISP	SCP domain-containing protein	15.8	*Micrurus corallinus*	A0A2D4G403	138	10	2	99.0%	191	0.3
NGF-beta	Venom nerve growth factor	13.4	*Naja atra*	P61898	116	34	10	99.0%	490	2.4
SVMP	Zinc metalloproteinase-disintegrin-like atragin	71.4	*Naja atra*	D3TTC2	613	63	20	99.0%	980	0.6
SVMP	Zinc metalloproteinase-disintegrin-like kaouthiagin-like	68.2	*Naja atra*	D3TTC1	593	44	17	99.0%	629	0.6
SVMP	Zinc metalloproteinase-disintegrin-like atrase-A	70.4	*Naja atra*	D5LMJ3	607	41	15	99.0%	526	0.2
SVMP	Zinc metalloproteinase-disintegrin-like mikarin (Fragments)	19.5	*Micropechis ikaheca*	P0DJ43	169	1	1	90.5%	15	<0.1
SVMP	SVMP-Den-9	70.5	*Denisonia devisi*	R4FIC4	613	7	1	83.9%	93	<0.1
SVMP	Metalloproteinase 12 (Fragment)	73.9	*Ahaetulla prasina*	A0A346CM42	614	2	2	98.5%	28	<0.1
UP	Uncharacterized protein (Fragment)	33.5	*Micrurus corallinus*	A0A2D4GFB1	291	9	1	81.8%	95	1.0

Table 1. Cont.

Family	Protein name	Protein mass (kDa)	Source organism	Database accession	Length	No. of peptide	No. of non-duplicate peptide	Probability	Score	Relative abundance (%)
UP	Uncharacterized protein (Fragment)	14.8	*Micrurus surinamensis*	A0A2D4Q7C6	131	4	3	99.0%	59	0.1
UP	Uncharacterized protein (Fragment)	18.8	*Ophiophagus hannah*	V8N885	157	3	3	99.0%	31	0.1
UP	Uncharacterized protein	40.5	*Micrurus corallinus*	A0A2D4FIT3	349	1	1	91.1%	15	<0.1
GLU	Glutathione peroxidase (Fragment)	29.8	*Ophiophagus hannah*	V8P395	264	20	8	99.0%	277	0.6
peptidase S1	Plasminogen activator	61.6	*Crotalus adamanteus*	A0A0F7Z9B1	526	11	6	99.0%	148	0.1
peptidase S1	Snake venom serine protease NaSP	31.9	*Naja atra*	A8QL53	282	4	3	99.0%	58	0.1
peptidase S1	Tissue-type plasminogen activator (Fragment)	32.5	*Ophiophagus hannah*	V8NYC7	283	3	2	99.0%	45	0.1
OV	Ohanin	23.7	*Phalotris mertensi*	A0A182C6D0	213	7	4	99.0%	89	0.2
OV	Ohanin	24.6	*Micrurus surinamensis*	A0A2D4NZ30	220	4	2	95.4%	40	0.1
PDE	Snake venom phosphodiesterase	96.4	*Naja atra*	A0A2D0TC04	830	50	29	99.0%	730	0.2
5'-NU	Ecto-5"-nucleotidase	63.7	*Micrurus tener*	A0A194AS98	574	32	16	99.0%	466	0.2
FMO	Amine oxidase (Fragment)	58.3	*Naja atra*	A0A2R4N4Q6	507	25	19	99.0%	352	0.1
ENDOD1	Endonuclease domain-containing 1 protein	19.8	*Ophiophagus hannah*	V8N4Y2	160	8	6	99.0%	114	0.2
MCM	DNA helicase	97.9	*Micrurus spixii*	A0A2D4MKN7	863	4	1	79.3%	40	0.1
PI3/PI4-kinase	Phosphatidylinositol-4,5-bisphosphate 3-kinase catalytic subunit delta isoform (Fragment)	27.3	*Ophiophagus hannah*	V8NEE1	235	22	1	83.8%	230	<0.1
S-100	Protein S100	10.3	*Boiga irregularis*	A0A0B8RWC4	90	1	1	89.8%	15	<0.1
S-100	Protein S100	10.2	*Micrurus fulvius*	U3FBA4	90	1	1	85.8%	13	<0.1
Type-B carboxylesterase/ lipase	Carboxylic ester hydrolase	69.0	*Ahaetulla prasina*	A0A346CLZ4	605	4	4	99.0%	53	<0.1
TMEM131	Transmembrane protein 131	182.2	*Crotalus adamanteus*	A0A0F7Z222	1592	2	2	95.3%	20	<0.1
PLBL	Phospholipase-B 81	64.4	*Drysdalia coronoides*	F8J2D3	553	2	2	99.0%	40	<0.1
Cystatin	Cystatin	16.1	*Naja kaouthia*	E3P6P4	141	2	1	92.7%	32	<0.1
CSA	Cobra serum albumin	71.7	*Naja naja*	Q91134	614	1	1	90.6%	17	<0.1

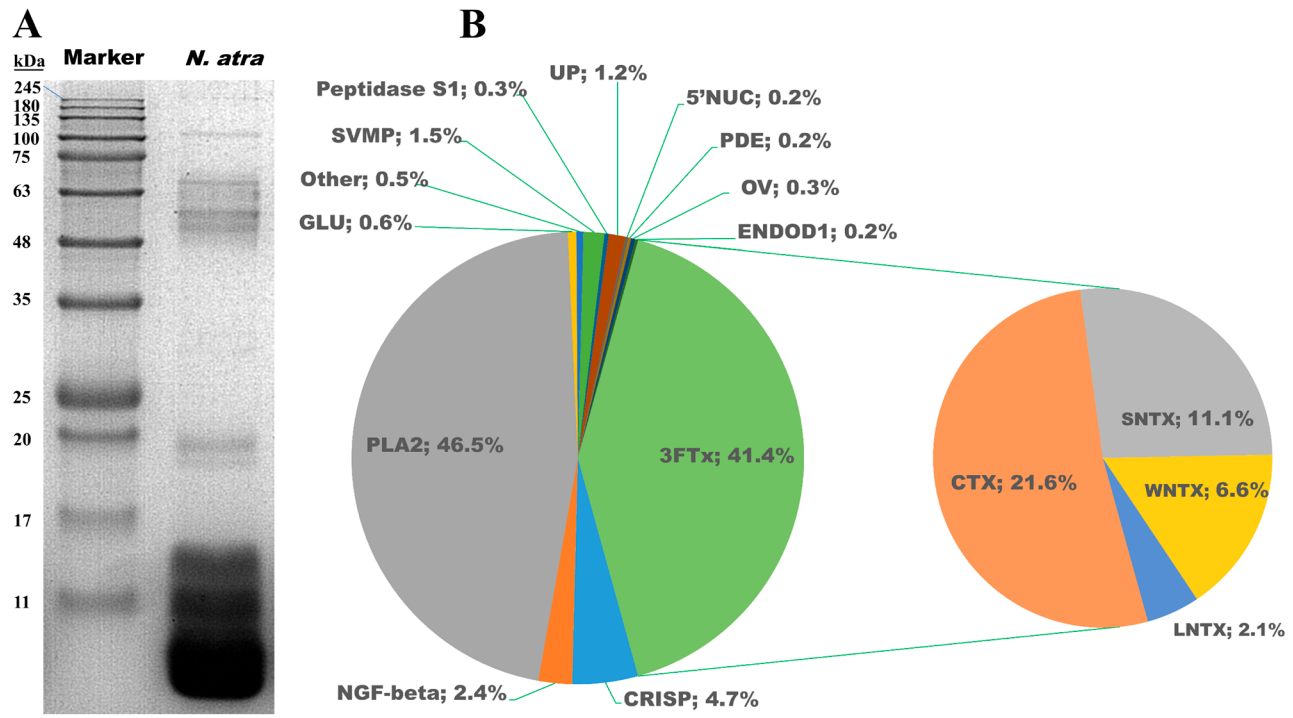

Figure 1. SDS-PAGE and proteomes of *N. atra* venom. **(A)** Protein separation of *N. atra* venom (20 μg) on 15% SDS-PAGE under reducing conditions. **(B)** Composition of *N. atra* venom according to protein families, expressed as percentages of the total protein content. *N. atra*: *Naja atra*; PLA $_2$: phospholipase A_2; 3FTx: three-finger toxin; CRISP: cysteine-rich secretory protein; NGF-beta: venom nerve growth factor; SVMP: snake venom metalloproteinase; PDE: phosphodiesterase; 5'NUC: 5'-nucleotidases; GLU: glutathione peroxidase; UP: uncharacterized protein; SNTX: short-chain α-neurotoxin; LNTX: long-chain α-neurotoxin; WNTX: weak neurotoxin.

Table 2. The median lethal dose (LD_{50}) of *N. atra* venom.

Venom dose (mg/kg, s.c.)	Dose logarithm	Number of mice	Number of dead mice	Mortality (%)
Control	–	10	0	0
0.5	–0.3010	10	0	0
0.7	–0.1549	10	2	20
1.1	0.0414	10	6	60
1.7	0.2304	10	9	90
2.5	0.3979	10	10	100

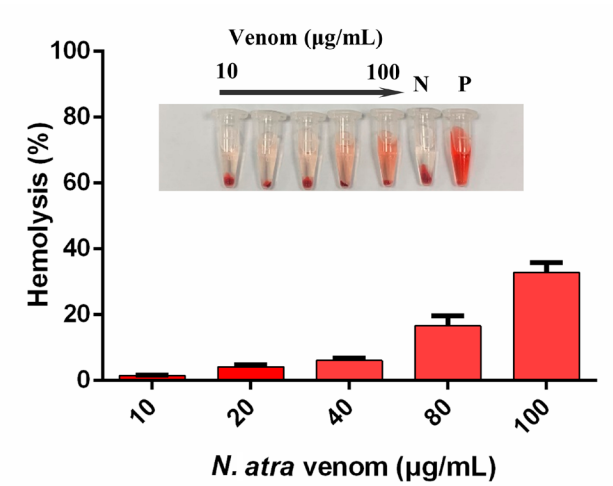

Figure 2. Direct hemolysis caused by *N. atra* venom in rabbit erythrocytes. N: negative control (saline); P: positive control (distilled water). Data are presented as mean ± SEM (n = 6 each).

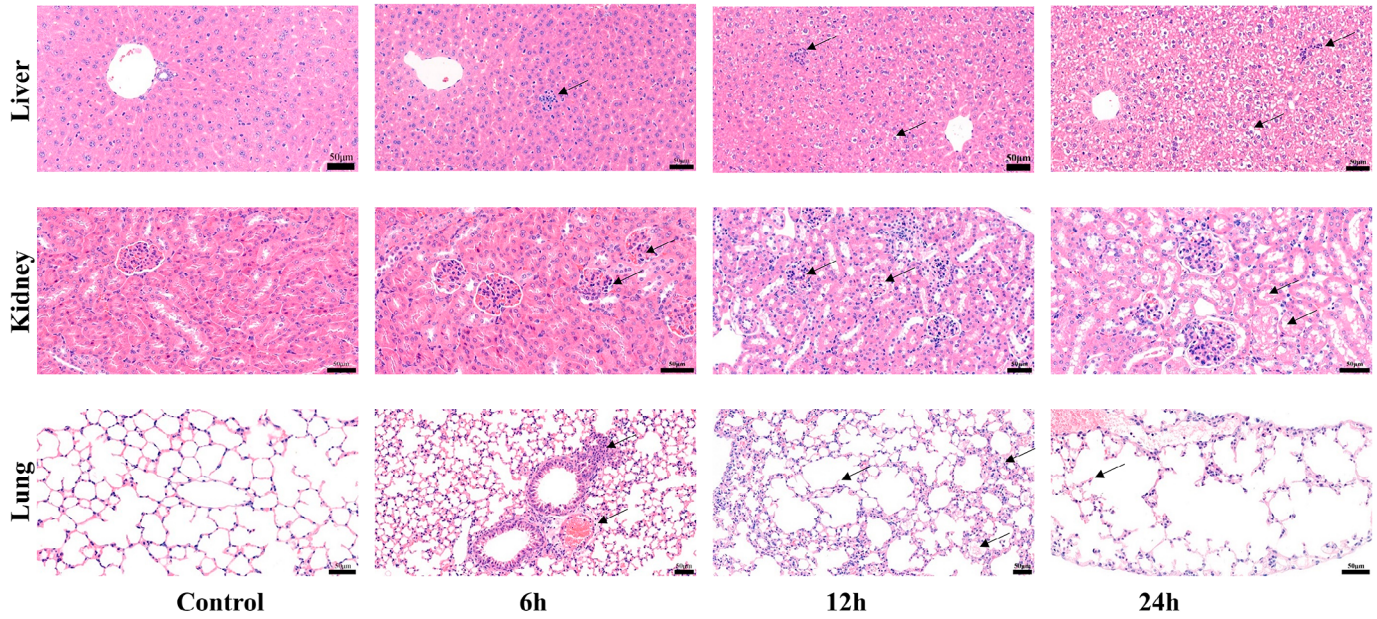

Figure 3. Histological analysis of hepatic, renal and pulmonary tissues of mice 6h, 12h and 24h after the injection of one LD_{50} (1.02 mg/kg, s.c.) of *N. atra* venom. The black arrows indicate the lesion area (scale bar: 50 μm).

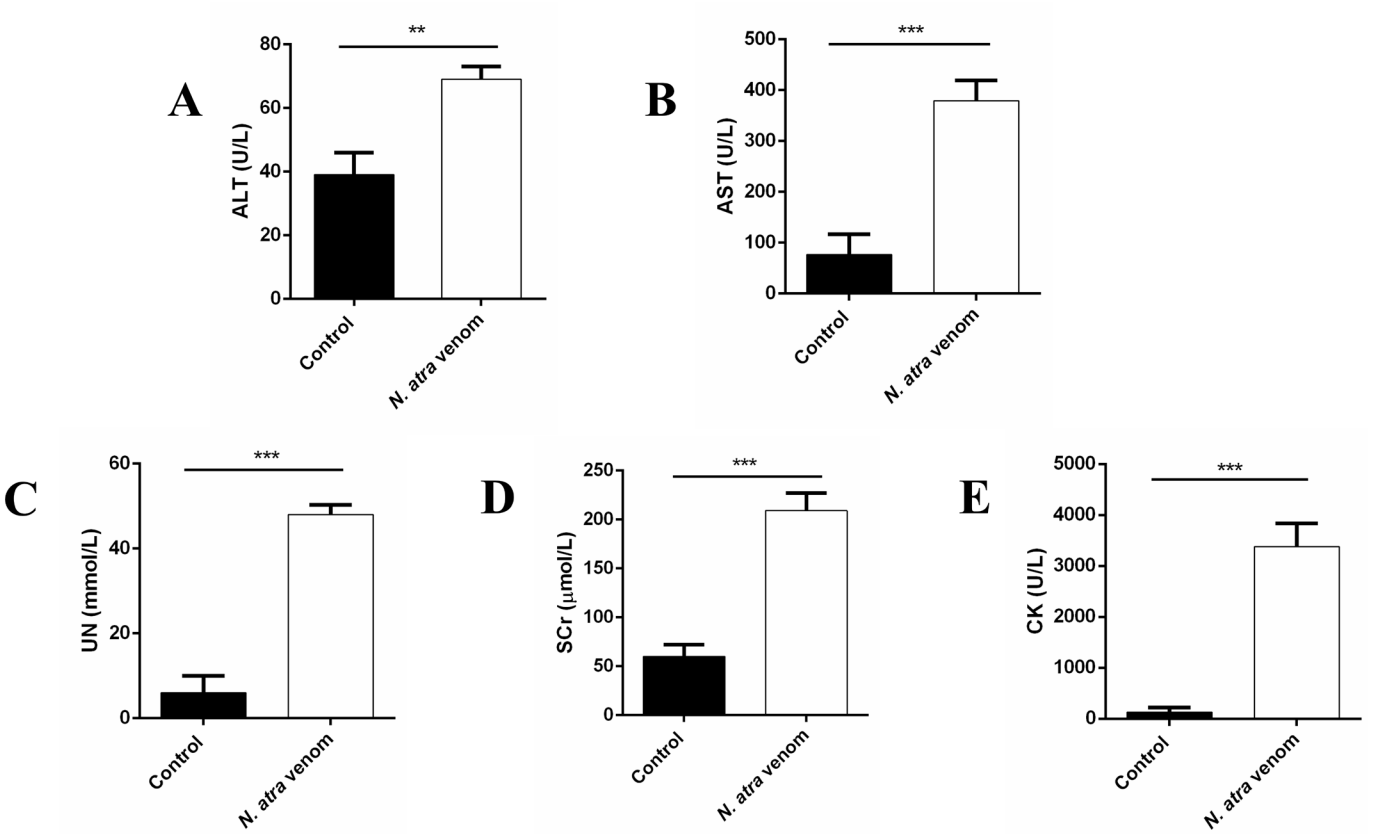

Figure 4. Increases in the serum **(A)** ALT, **(B)** AST, **(C)** UN, **(D)** SCr and **(E)** CK levels of mice 1h after the injection of one LD_{50} (1.02 mg/kg, s.c.) of *N. atra* venom. The columns represent the mean +/- SEM (n = 6 each). **p < 0.01 and **p < 0.001.

Discussion

With growing demand for snake venom products, the economic and medicinal value of snake venom is becoming more and more prominent. However, the hidden danger is that intraspecific variation in venom composition may affect the clinical pathophysiology of envenomation, venom toxicity, and the function of venom products [23]. Hence, understanding the compositional and toxicological properties of snake venom from completely different regions is crucial. Importantly, venom used in this study was collected from the same group of snakes living in the same conditions, which is vital to guarantee a quality sample for this research [24].

In this study, SDS-PAGE of *N. atra* venom samples showed the presence of prominent protein bands, similar to those previously reported [4,7,8,10] and also similar to those documented for other elapids, including *Naja* and *Bungarus caeruleus* [25]. The venom proteomic results obtained here based on direct tryptic digestion supported this hypothesis. Similar to the proteomic profile of *N. atra* venom from other regions, such as Taiwan and Zhejiang province, China, venom proteins consisted mainly of 3FTx and PLA_2 [2,8,26,27]. However, the relative abundances of these two families of toxins were not significantly different from each other, in contrast to previous studies [2,8,26]. Geographic variation in *N. atra* venom proteomic profiles has been observed, with 3FTx showing a surprising geographical variation [8]. However, these studies have focused mainly on factors that influence venom variation, an aspect that we did not address in our study. Future studies should examine the factors that influence intraspecific variation in venom composition and the mechanisms involved.

Consistent with previous work, the main component of 3FTx in *N. atra* venom is cytotoxin, known as cardiotoxin, followed by short chain α-neurotoxin, weak neurotoxin and long chain neurotoxin [2,8,28]. Cytotoxins are the principal toxic components that cause hemolytic damage, membrane disruption, and circulatory failure [29]. Cardiotoxin isolated from *N. atra* venom induces direct hemolysis in washed erythrocytes from several animals [30]. Although we were unable to identify a single specific component of venom for inducing hemolysis, we did find that *N. atra* venom induce direct hemolysis in rabbit erythrocytes in the present study, unlike other cobra venoms [31].

Furthermore, the short-chain α-neurotoxin (type I α-neurotoxin) toxin of 3FTx in this venom binds to the muscle nAChR and inhibits the binding of acetylcholine to its receptor, thereby impairing neuromuscular transmission [32]. Orphan group II toxins showed weak α-neurotoxin activity. Long-chain α-neurotoxin (type II α-neurotoxin) of 3FTx is a peripheral nAChR antagonist that causes paralysis, respiratory failure, and death [33,34]. Overall, based on venom proteomics, *N. atra* venom would exhibit strong neurotoxicity in experimental animals [2]. In agreement with this, the lethality assay showed that the s.c. injection of *N. atra* venom caused muscle weakness and respiratory paralysis. However, for humans, neurotoxic symptoms do not seem to be a clinically vital consequence of *N. atra* envenomation [3]. The reason for the discrepancy between neurotoxic effects of *N. atra* envenomation in mice and humans remain unclear. Moreover, the LD_{50} of venom in the present study was 1.02 mg/kg, which was higher than that of venom samples collected from Zhejiang (0.68 mg/kg, s.c.) and Taiwan (0.29 mg/kg, s.c.) [2,8]. Although the origin of the venom is different, the lethal dose of venom in this study was higher than that of other regions, suggesting that it might be less lethal.

PLA_2 is the most abundant component of venom in this study, indicating that it may be an important factor in the pathogenesis of *N. atra* envenomation. PLA_2 exert multiple toxic effects on the prey or victim, such as membrane damage, myotoxicity, neurotoxicity, and edema [35,36]. Moreover, PLA_2 has also been implicated in multiple pathologies, including hepatotoxicity and nephrotoxicity [37]. Additionally, PLA_2 from *Naja kaouthia* venom has been reported to promote CTX-induced cytotoxicity in cell models, leading to cell vacuolation and rupture [27], which indicates that cobra PLA_2 play a role in the pathogenesis of necrosis. *N. atra* venom triggered considerable cell necrosis in the hepatic, renal and pulmonary tissues of mice in this study, which was similar to the findings reported for venom collected from other cobra species [38,39]. Importantly, the significant changes in serum biochemical parameters observed here indicated that *N. atra* venom caused damage to the liver, kidney, and lung of the mice.

Myonecrosis is a common phenomenon in animals injected with snake venom [40]. As shown in the present study, a significant increase in serum levels of CK also indicated that skeletal and cardiac muscle necrosis occurred in the mice injected with *N. atra* venom, and similar activity was reported in other studies conducted on different types of snake venom [41–43]. Several previous studies have reported the occurrence of muscle fiber degeneration after the injection of cardiotoxin from *N. atra* [44–46], which is similar to the pathological analysis results of heart tissue obtained in the present study. The study of *Naja* venom is important due to its great potential for medical application as an anticancer among others [47].

Conclusion

In conclusion, the present study investigated the components of farm-raised *N. atra* venom and assessed its toxicity *in vivo* and *in vitro*. This work extends our knowledge regarding venom of farm-raised *N. atra,* indicating that PLA_2 and 3FTx are major protein families in venom that exhibit direct hemolytic activity, neurotoxicity, myotoxicity, and induce pathological changes in tissues. These findings provide information on the venom of captive *N. atra* from Hunan province, China, that should be useful in future comparisons with venom from wild snakes from the same geographic region.

Abbreviations

3FTx: three-finger toxin; 5'NUC: 5'-nucleotidases; ALT: alanine aminotransferase; AST: aspartate aminotransferase; CID:

collision induced dissociation; CK: creatine kinase; CRISP: cysteine-rich secretory protein; CSA: cobra serum albumin; CVF: cobra venom factor; ddH_2O: double distilled H_2O; DTT: dithiothreitol; HPLC, high-pressure liquid chromatography; ENDOD1: endonuclease domain-containing 1 protein; ESI: electrospray ionization; FMO: flavin monoamine oxidase; GLU: glutathione peroxidase; H&E: hematoxylin and eosin; KUN: Kunitz-type serine protease inhibitors; LAAO: L-amino acid oxidase; LD_{50}: median lethal dose; LNTX: long-chain α-neurotoxin; *N. atra*: *Naja atra*; Nano-LC-ESI-MS/MS: nano liquid chromatography with electrospray ionization tandem mass spectrometry; OV: ohanin/vespryn; PDE: phosphodiesterase; PLA_2: phospholipase A_2; PLBL: phospholipase B-like; SCr: serum creatine; SDS-PAGE: sodium dodecyl sulfate-polyacrylamide gel electrophoresis; SNTX: short-chain α-neurotoxin; SVMP: snake venom metalloproteinase; UN: urea nitrogen; UP: uncharacterized protein; WNTX: weak neurotoxin.

Availability of data and materials

All data generated or analyzed during this study are included in this article. The mass spectrometry proteomics data were deposited in the ProteomeXchange Consortium (http://proteomecentral.proteomexchange.org) via the iProX partner repository [48] with the dataset identifier PXD027140.

Funding

Not applicable.

Competing interests

The authors declare that they have no competing interests.

Authors' contributions

GX, JQL and ZLS conceived and designed the experiments. GX, JQL, LFP and YY performed the experiments and analyzed the data. GX wrote the paper, which was edited by JQL, ZLS and YY. All authors read and approved the final manuscript.

Ethics approval

The animal study protocol of the present work was approved by the Ethics Committee of Hunan Agricultural University (process n. 43321503).

Consent for publication

Not applicable.

Supplementary material

The following online material is available for this article:

Additional file 1. Identification results of nano-LC-ESI-MS/MS protein spectrum of *N. atra* venom.

Additional file 2. Histological analysis of heart tissue from mice 24h after the injection of one LD50 (1.02 mg/kg, s.c.) of N. atra venom. The black arrows indicate the lesion area (scale bar: 50 μm).

References

1. Qin GP. China poisonous snake research. 2d ed. Qin GP, editor. Nanning (China): Guangxi Science and Technology Publishing House; 1998.
2. Liu CC, Chou YS, Chen CY, Liu KL, Huang GJ, Yu JS, Wu CJ, Liaw GW, Hsieh CH, Chen CK. Pathogenesis of local necrosis induced by *Naja atra* venom: Assessment of the neutralization ability of Taiwanese freeze-dried neurotoxic antivenom in animal models. PLoS Negl Trop Dis. 2020 Feb 7;14(2):e0008054.
3. Mao YC, Liu PY, Chiang LC, Lai CS, Lai KL, Ho CH, Wang TH, Yang CC. *Naja atra* snakebite in Taiwan. Clin Toxicol (Phila). 2017 Apr 56(4):273-80.
4. He Y, Gao JF, Lin LH, Ma XM, Ji X. Age-related variation in snake venom: Evidence from two snakes (*Naja atra* and *Deinagkistrodon acutus*) in southeastern China. Asian Herpetol Res. 2014 Jun 25;5(2):119-27.
5. Liang Q, Huynh TM, Isbister GK, Hodgson WC. Isolation and pharmacological characterization of α-Elapitoxin-Na1a, a novel short-chain postsynaptic neurotoxin from the venom of the Chinese Cobra (*Naja atra*). Biochem Pharmacol. 2020 Nov 181:114059.
6. Fu C, Shi L, Huang X, Feng H, Tan X, Chen S, Zhu L, Sun QY, Chen G. Atrase B, a novel metalloprotease with anti-complement and anti-coagulant activity, significantly delays discordant cardiac xenograft rejection. Xenotransplantation. 2020 Sep 27(5):e12616.
7. Liu CC, Lin CC, Hsiao YC, Wang PJ, Yu JS. Proteomic characterization of six Taiwanese snake venoms: Identification of species-specific proteins and development of a SISCAPA-MRM assay for cobra venom factors. J Proteomics. 2018 Sep 15;187:59-68.
8. Huang HW, Liu BS, Chien KY, Chiang LC, Huang SY, Sung WC, Wu WG. Cobra venom proteome and glycome determined from individual snakes of *Naja atra* reveal medically important dynamic range and systematic geographic variation. J Proteomics. 2015 Oct 14;128:92-104.
9. Jiang Y, Li Y, Lee W, Xu X, Zhang Y, Zhao R, Zhang Y, Wang W. Venom gland transcriptomes of two elapid snakes (*Bungarus multicinctus* and *Naja atra*) and evolution of toxin genes. BMC Genomics. 2011 Jan 3;12:1.
10. Li S, Wang J, Zhang X, Ren Y, Wang N, Zhao K, Chen X, Zhao C, Li X, Shao J, Yin J, West MB, Xu N, Liu S. Proteomic characterization of two snake venoms: *Naja naja atra* and *Agkistrodon halys*. Biochem J. 2004 Nov 15;384(Pt 1):119-27.
11. Gao JF, Yin Y, Qu YF, Wang J, Lin LH, Lu HL, Ji X. Identifying intraspecific variation in venom yield of Chinese Cobra (*Naja atra*) from ten populations in mainland China. Asian Herpetol Res. 2019 May;10(1):32-40.
12. Farias IB, Morais-Zani K, Serino-Silva C, Sant'Anna SS, Rocha M, Grego KF, Andrade-Silva D, Serrano SMT, Tanaka-Azevedo AM. Functional and proteomic comparison of *Bothrops jararaca* venom from captive specimens and the Brazilian Bothropic Reference Venom. J Proteomics. 2018 Mar 1;174:36-46.
13. Oh AMF, Tan CH, Ariaranee GC, Quraishi N, Tan NH. Venomics of *Bungarus caeruleus* (Indian krait): Comparable venom profiles, variable immunoreactivities among specimens from Sri Lanka, India and Pakistan. J Proteomics. 2017 Jul 5;164:1-18.
14. Reeks T, Lavergne V, Sunagar K, Jones A, Undheim E, Dunstan N, Fry B, Alewood PF. Deep venomics of the *Pseudonaja* genus reveals inter- and intra-specific variation. J Proteomics. 2016 Feb 5;133:20-32.
15. Sintiprungrat K, Watcharatanyatip K, Senevirathne WDST, Chaisuriya P, Chokchaichamnankit D, Srisomsap C, Ratanabanangkoon K. A comparative study of venomics of *Naja naja* from India and Sri Lanka, clinical manifestations and antivenomics of an Indian polyspecific antivenom. J Proteomics. 2016 Jan 30;132:131-43.
16. Gao JF, Qu YF, Zhang XQ, Ji X. Within-clutch variation in venoms from hatchlings of *Deinagkistrodon acutus* (Viperidae). Toxicon. 2011 Jun;57(7-8):970-7.

17. Beraldo Neto E, Coelho GR, Sciani JM, Pimenta DC. Proteomic characterization of *Naja mandalayensis* venom. J Venom Anim Toxins incl Trop Dis. 2021 Jul 27:e20200125. https://doi.org/10.1590/1678-9199-JVATITD-2020-0125.
18. Laemmli UK. Cleavage of structural proteins during the assembly of the head of bacteriophage T4. Nature. 1970 Aug 15;227(5259):680-5.
19. Shevchenko A, Wilm M, Vorm O, Mann M. Mass spectrometric sequencing of proteins silver-stained polyacrylamide gels. Anal Chem. 1996 Mar 1;68(5):850-8.
20. Griffin NM, Yu J, Long F, Oh P, Shore S, Li Y, Koziol JA, Schnitzer JE. Label-free, normalized quantification of complex mass spectrometry data for proteomic analysis. Nat Biotechnol. 2010 Jan;28(1):83-9.
21. Accary C, Hraoui-Bloquet S, Hamze M, Mallem Y, El Omar F, Sabatier JM, Desfontis JC, Fajloun Z. Protein content analysis and antimicrobial activity of the crude venom of *Montivipera bornmuelleri*; a viper from Lebanon. Infect Disord Drug Targets. 2014 May;14(1):49-55.
22. Finney DJ. Probit analysis : a statistical treatment of the sigmoid response curve. 2d ed. Finney DJ, editor. Cambridge (England): University Press; 1952.
23. Grego KF, Vieira SEM, Vidueiros JP, Serapicos EO, Barbarini CC, da Silveira GPM, Rodrigues FD, Alves LDF, Stuginski DR, Rameh-de-Albuquerque LC. Maintenance of venomous snakes in captivity for venom production at Butantan Institute from 1908 to the present: a scoping history. J Venom Anim Toxins incl Trop Dis. 2021 Jan;27:e20200068. https://doi.org/10.1590/1678-9199-JVATITD-2020-0068.
24. Santos L, Oliveira C, Vasconcelos BM, Vilela D, Melo L, Ambrosio L, Silva A, Murback L, Kurissio J, Cavalcante J, Cassaro CV, Barros L, Barraviera B, Ferreira Jr RS. Good management practices of venomous snakes in captivity to produce biological venom-based medicines: achieving replicability and contributing to pharmaceutical industry. J Toxicol Environ Health B Crit Rev. 2021 Jan 2;24(1):30-50.
25. Choudhury M, McCleary RJR, Kesherwani M, Kini RM, Velmurugan D. Comparison of proteomic profiles of the venoms of two of the 'Big Four' snakes of India, the Indian cobra (*Naja naja*) and the common krait (*Bungarus caeruleus*), and analyses of their toxins. Toxicon. 2017 Sep 1;135:33-42.
26. Shan LL, Gao JF, Zhang YX, Shen SS, He Y, Wang J, Ma XM, Ji X. Proteomic characterization and comparison of venoms from two elapid snakes (*Bungarus multicinctus* and *Naja atra*) from China. J Proteomics. 2016 Apr 14;138:83-94.
27. Gasanov SE, Alsarraj MA, Gasanov NE, Rael ED. Cobra venom cytotoxin free of phospholipase A_2 and its effect on model membranes and *T leukemia* cells. J Membr Biol. 1997 Jan 15;155(2):133-42.
28. Liu CC, You CH, Wang PJ, Yu JS, Huang GJ, Liu CH, Hsieh WC, Lin CC. Analysis of the efficacy of Taiwanese freeze-dried neurotoxic antivenom against *Naja kaouthia*, *Naja siamensis* and *Ophiophagus hannah* through proteomics and animal model approaches. PLoS Negl Trop Dis. 2017 Dec 15;11(12):e0006138.
29. Suzuki-Matsubara M, Athauda SB, Suzuki Y, Matsubara K, Moriyama A. Comparison of the primary structures, cytotoxicities, and affinities to phospholipids of five kinds of cytotoxins from the venom of Indian cobra, *Naja naja*. Comp Biochem Physiol C Toxicol Pharmacol. 2016 Jan;179:158-64.
30. Troiano JC GE, Gould I. Gould I. Hemolitic action of *Naja naja atra* cardiotoxin on erythrocytes from different animals. J Venom Anim Toxins incl Trop Dis. 2006 Oct;12(1). https://doi.org/10.1590/S1678-91992006000100004.
31. Das D, Urs N, Hiremath V, Vishwanath BS, Doley R. Biochemical and biological characterization of *Naja kaouthia* venom from North-East India and its neutralization by polyvalent antivenom. J Venom Res. 2013 Nov 6;4:31-8.
32. Ismail M, Aly MH, Abd-Elsalam MA, Morad AM. A three-compartment open pharmacokinetic model can explain variable toxicities of cobra venoms and their alpha toxins. Toxicon. 1996 Sep;34(9):1011-26.
33. Kini RM, Doley R. Structure, function and evolution of three-finger toxins: mini proteins with multiple targets. Toxicon. 2010 Nov;56(6):855-67.
34. Fry BG, Wuster W, Kini RM, Brusic V, Khan A, Venkataraman D, Rooney AP. Molecular evolution and phylogeny of elapid snake venom three-finger toxins. J Mol Evol. 2003 Jul;57(1):110-29.
35. Cordeiro FA, Perini TG, Bregge-Silva C, Cremonez CM, Rodrigues RS, Boldrini-Franca J, Bordon Kde C, De Souza DL, Ache DC, Rodrigues VM, Santos WFS, Rosa JC, Arantesa EC. A New Phospholipase A(2) from *Lachesis muta rhombeata*: Purification, Biochemical and Comparative Characterization with Crotoxin B. Protein Pept Lett. 2015 Jul;22(9):816-27.
36. Carvalho BM, Santos JD, Xavier BM, Almeida JR, Resende LM, Martins W, Marcussi S, Marangoni S, Stabeli RG, Calderon LA, Soares AM, da Silva SL, Marchi-Salvador DP. Snake venom PLA2s inhibitors isolated from Brazilian plants: synthetic and natural molecules. Biomed Res Int. 2013 Sep;2013:153045.
37. Al-Asmari AK, Khan HA, Manthiri RA, Al-Khlaiwi AA, Al-Asmari BA, Ibrahim KE. Protective effects of a natural herbal compound quercetin against snake venom-induced hepatic and renal toxicities in rats. Food Chem Toxicol. 2018 Aug;118:105-10.
38. Rahmy TR, Hemmaid KZ. Histological and histochemical alterations in the liver following intramuscular injection with a sublethal dose of the *Egyptian cobra* venom. J Nat Toxins. 2000 Feb;9(1):21-32.
39. Rahmy TR. Effects of intramuscular injection of a sublethal dose of the *Egyptian cobra* snake on the histological and histochemical pattern of the kidney. J Nat Toxins. 2000 May;9(2):159-78.
40. Mamede CCN, de Sousa Simamoto BB, da Cunha Pereira DF, de Oliveira Costa J, Ribeiro MSM, de Oliveira F. Edema, hyperalgesia and myonecrosis induced by Brazilian bothropic venoms: overview of the last decade. Toxicon. 2020 Nov;187:10-8.
41. Xu N, Zhao HY, Yin Y, Shen SS, Shan LL, Chen CX, Zhang YX, Gao JF, Ji X. Combined venomics, antivenomics and venom gland transcriptome analysis of the monocled cobra (*Naja kaouthia*) from China. J Proteomics. 2017 Apr;21;159:19-31.
42. Nourreddine FZ, Oussedik-Oumehdi H, Laraba-Djebari F. Myotoxicity induced by *Cerastes cerastes* venom: Beneficial effect of heparin in skeletal muscle tissue regeneration. Acta Trop. 2020 Feb;202:105274.
43. Reis LPG, Botelho AFM, Novais CR, Fiuza ATL, Barreto MSO, Ferreira MG, Bonilla C, Chavez-Olortegui C, Melo MM. Cardiotoxic effects of *Micrurus surinamensis* (Cuvier, 1817) snake venom. Cardiovasc Toxicol. 2021 Jun;21(6):462-71.
44. Ownby CL, Fletcher JE, Colberg TR. Cardiotoxin 1 from cobra (*Naja naja atra*) venom causes necrosis of skeletal muscle *in vivo*. Toxicon. 1993 Jun;31(6):697-709.
45. Vignaud A, Hourde C, Butler-Browne G, Ferry A. Differential recovery of neuromuscular function after nerve/muscle injury induced by crude venom from *Notechis scutatus*, cardiotoxin from *Naja atra* and bupivacaine treatments in mice. Neurosci Res. 2007 Jul;58(3):317-23.
46. Standker L, Harvey AL, Furst S, Mathes I, Forssmann WG, Escalona de Motta G, Beress L. Improved method for the isolation, characterization and examination of neuromuscular and toxic properties of selected polypeptide fractions from the crude venom of the Taiwan cobra *Naja naja atra*. Toxicon. 2012 Sep 15;60(4):623-31.
47. Attarde SS, Pandit SV. Anticancer potential of nanogold conjugated toxin GNP-NN-32 from Naja naja venom. J Venom Anim Toxins incl Trop Dis. 2020 Mar 2;26:e20190047. https://doi.org/10.1590/1678-9199-JVATITD-2019-0047.
48. Ma J, Chen T, Wu S, Yang C, Bai M, Shu K, Li K, Zhang G, Jin Z, He F, Hermjakob H, Zhu Y. iProX: an integrated proteome resource. Nucleic Acids Res. 2019 Jan 8;47(D1):D1211-7.